The Cryosphere Discuss., 4, 1011–1034, 2010
www.the-cryosphere-discuss.net/4/1011/2010/
doi:10.5194/tcd-4-1011-2010

The Cryosphere Discussions

Cryogenic and non-cryogenic pool calcites reflect alternating permafrost and interglacial periods (Breitscheid-Erdbach Cave, Germany)

D. K. Richter[1], P. Meissner[1], A. Immenhauser[1], U. Schulte[1], and I. Dorsten[2]

[1]Ruhr-University Bochum, Institute for Geology, Mineralogy and Geophysics, Universitätsstr. 150, 44801 Bochum, Germany
[2]Am Schleidt 9, 35745 Herborn, Germany

Received: 4 June 2010 – Accepted: 11 June 2010 – Published: 15 July 2010

Correspondence to: D. K. Richter (detlev.richter@rub.de)

Published by Copernicus Publications on behalf of the European Geosciences Union.

Abstract

Weichselian cryogenic calcites collected in what is referred to as the "Rätselhalle" of the Breitscheid-Erdbach Cave were structurally classified as rhombohedral crystal and spherulitic crystal sinters. The carbon and oxygen isotopic composition of these precipitates corresponds to those of known cryogenic calcites of slow genesis of Central European caves (δ^{13}C=+0.6 and −7.3‰; δ^{18}O=−6.9 to −18.0‰). The variant carbon and oxygen isotope pattern differing between different caves is attributed to cave specific ventilation. Particularly, Breitscheid cryogenic calcites reflect mean levels of cave ventilation. By petrographic and geochemical comparisons of Weichselian cryogenic calcite with recent to sub-recent precipitates as well as Weichselian non-cryogenic calcites of the same locality, a model for the precipitation of these calcites is proposed. While the recent and sub-recent pool-calcites isotopically match the geochemistry of interglacial speleothems (stalagmites, etc.), isotope ratios of Weichselian non-cryogenic pool-calcites reflect cooler conditions. Weichselian cryogenic calcites show a trend towards ^{18}O-depleted values with higher carbon isotope ratios reflecting slow freezing of the precipitating solution. In essence, the isotope geochemistry of the Weichselian calcites reflects the climate history changing from overall initial permafrost (glacial) conditions to an interglacial and subsequently to renewed permafrost conditions. The last stage then grades into the present-day warm period. Judging from the data compiled here, the last permafrost stage is followed by only one interglacial. During this interglacial, the cave ice melted and non-cryogenic Weichselian calcite precipitates were deposited on the cave ground or on fallen blocks, respectively.

1 Introduction

Cryogenic cave calcites (CCC sensu Žák et al., 2004) form during freezing of carbonate saturated cave waters. This process takes place when seepage waters enter a cave or cave system characterized by mean temperatures below 0 °C. Alternatively,

TCD
4, 1011–1034, 2010

the 0 °C isotherm might fluctuate over time. Due to evaporation effects, rapid freezing of cave waters leads to ^{13}C-enriched values of precipitated calcites (Lacelle, 2007; Spötl, 2008). In contrast, slowly freezing waters and related preferential ^{18}O incorporation into the ice, leads to a low δ^{18}O of calcite precipitates from this fluid (Žák et al.,2004).

In recent years, Quaternary cryogenic calcites formed by slow growth conditions from Central European caves were described in a series of publications (locations between Scandinavian and Alpine ice shields; Žák et al., 2004, 2008; Richter and Niggemann, 2005; Richter and Riechelmann, 2008; Richter et al., 2008, 2009). The genesis of these calcite particles is essentially bound to water pools on top of ice bodies in caves during the transition periods between warm and cold periods. Conversely, the precipitation of similar calcites from pool waters on the cave floor is not yet documented. Nevertheless, during these transition periods, mean annual temperatures outside of the cave gradually decrease and then fall below the freezing point. Following a subsequent temperature warming, cave ice, formed during cold periods, melts and different types of cryogenic calcites are accumulated on the cave ground or on collapsed blocks covering the cave floor.

Unconsolidated sediments of calcite particles with a broad range of structures are locally accumulated on the cave floor and on blocks in the "Rätselhalle" of the Breitscheid-Erdbach Cave in NW Hesse ("Herbstlabyrinth-Advent" cave system sensu Grubert (1996) and Hülsmann (1996); for location refer to Fig. 1). These deposits were sampled in 2004 and 2009 for detailed structural and geochemical analysis and are the topic of this present publication.

The age of the main type of the calcite particles found, namely aggregates of euhedral calcite crystals, was dated 29 170 ± 480 yrs based on the U/Th method (Kempe et al., 2005). These precipitates were interpreted as having formed as rafts on pool water situated on cave ice bodies (Kempe, 2008). The less commonly found types of calcite aggregates, here referred to as composite spherulites, were petrographically compared with known cryogenic calcites described by Richter and Niggemann (2005). The later ones were attributed to a precipitation setting in slowly freezing pools on ice

TCD
4, 1011–1034, 2010

bodies due to their ^{18}O depleted signature (−14 to −18‰ VPDB).

The genetic relation between before-mentioned types of "crystal sands" present in the "Rätselhalle" was previously poorly constrained. Here, the petrographic and geochemical properties of the different types of these crystal sands are documented in detail and a contrast comparison with recent/subrecent calcite formations in a sinter basin of the "Rätselhalle" is presented. The aim of this publication is to improve the understanding of cryogenic calcites as novel archives of cold continental climate phases.

2 Geographical and geological setting

The "Breitscheid-Erdbach" Cave formed in the Upper Devonian Iberger Limestone of Breitscheid (Kayser, 1907; Krebs, 1966) on the NE margin of the Tertiary Westerwald vulcanite (Fig. 1). The reefal deposits of the Iberger Limestone, located on a volcano basement in the Rhenoherzynic trough of the Rhenish Slate Mountains (Krebs, 1971), is well known for its abundant upper Cenozoic karst phenomena (Stengel-Rutkowski, 1968). Conversely, the "Herbstlabyrinth-Adventhöhlen" cave system was first discovered in winter of 1993/94 during quarry works (Grubert, 1996). Following Dorsten et al., (2005), this cave system formed in a shallow phreatic system. Several of the cave levels reflect the palaeo-position of ancient long-lasting ground water tables. Kaiser et al. (1998) identified four karst levels, which today are situated in the vadose zone, and three subsequent stages of sinter formation have been identified but not yet dated. The "Herbstlabyrinth-Adventhöhlen" cave system is located between the villages of Erdbach and Breitscheid (Fig. 2). With an overall length of more than 5300 m, it is the largest cave system in Hesse and one of the most significant ones in Germany. The "Rätselhalle" (altitude 363 m a.s.l.) providing the sampling material for this study belongs to the western part of the EW trending main cave area. The thickness of the hostrock above the "Rätselhalle" reaches about 31 m.

TCD
4, 1011–1034, 2010

3 Methodology

"Crystal sand" accumulations covering the cave floor or lying on collapsed blocks (Figs. 3 and 4) were sampled at five locations. In addition, specimens of recent and sub-recent rafts of sinter deposits in a pool located in the NW-part of the "Rätselhalle" (Fig. 4) were collected for comparative studies.

The sample material was cleaned in an ultrasonic bath in the laboratory prior to a manual separation of the various sinter types under the binocular. The detailed external structure of small sinter precipitates was photographed under a high-resolution field emission scanning electron microscope (HR-FEM) of type LEO/Zeiss 1530 Gemini. For this purpose, selected samples have been sputtered with a thin gold coating. X-ray analysis (XRD) of the carbonate phases was performed with a Philips counting-tube diffractometer (PW 1050/25) with an AMR monochromator using CuK_α radiation (40 kV, 35 mA) in order to establish the carbonate mineralogy. For this, ground samples with quartz powder as internal standard have been measured in a diffraction angle range of 26–38°2θ, identifying each d(104) value of the rhombohedral carbonates in terms of their Ca/Mg distribution (Füchtbauer and Richter, 1988).

Carbon and oxygen isotopic compositions of calcite were determined with a delta S mass spectrometer (Finnigan MAT) and calibrated against V-PDB (Standards: CO-1 and CO-8). The 1σ-reproducibility of the measurements is 0.04‰ V-PDB for δ^{13}C and 0.08‰ V-PDB for δ^{18}O.

4 Data presentation and interpretation

4.1 Small sinter precipitates

Samples of small sinter precipitates are composed of nearly stoichiometric calcite (d(104) 3.034–3.036 Å) as documented by diffractometre analysis. This outcome is not unexpected given that the host rock of the cave is mainly composed of low Mg-

TCD
4, 1011–1034, 2010

calcite (d(104) 3.030–3.034 Å). Only small amounts of secondary dolomite are present in the hostrock carbonate. Below, small sinter precipitates sampled from the (i) cave floor and collapsed blocks and (ii) from sinter basins are described separately. This because differential formation models are proposed as based on field observations.

Small sinter precipitates collected from the cave floor and collapsed blocks

The most common form of small sinter precipitates are *rhombohedral crystal sinters*. These occur mostly as aggregates and subordinated as individual crystals at all sampling points (Fig. 4). In essence, two types are identified. These are (a) translucent, crystal sinters with acute rhombohedral faces on the edges and obtuse rhombohedral faces at their growth termination and (b) white to buff-colored, rhombohedral crystal sinters. Below the two types are described:

Translucent, rhombohedral crystal sinters (type a) with acute rhombohedral faces on the flanks and obtuse rhombohedral faces at their growth termination (Fig. 5a and b) are accumulated in many places over the study area. Commonly, rhombohedra are connected to platy crystallites approaching more than 1 cm in size. In most cases one side of these platy crystallites is commonly straight but also curved ones are found (Fig. 5c). The opposite side of platy aggregates is commonly convex and covered by euhedral crystals (Fig. 5a). Less common there are platy crystallites with euhedral crystals on both sides (Fig. 6a and b) reflecting sunken rafts of a former sinter basin. Asteroidal intergrowth of the rhombohedra is uncommon (up to >1 mm in diameter) whereas individual rhombohedra are rare (<1 mm in diameter).

White to buff-colored, rhombohedral crystal sinters (type b) were exclusively observed at location 1 (Fig. 4). They commonly occur as aggregates of up to 1 cm in diameter (Fig. 5e) but rare examples of single crystals were found too (Fig. 5d). The inclusion-rich rhombohedra display pronounced zoning and, where fully developed, curved crystal faces, which are less acute relative to the before-mentioned translucent type a rhombohedra. Type b frequently overgrows nuclei of type a (Figs. 5f and 6c, d).

TCD
4, 1011–1034, 2010

At locality 1 (Fig. 4), and only there, *spherulitic crystal sinters* are frequently found. These have a more white to buff-coloured appearance as a result of inclusions (see type b above) and rarely exceed 1 mm in size. Most spherulites are dumbbell-shaped and display complex intergrowth features (Fig. 5g). Chainlike linked spherulites ("braid sinter" sensu Erlemeyer et al., 1991; Richter et al., 2008) are not commonly found (Fig. 5h). Similar to rhombohedral crystal sinters of type b, rhombohedra display a curved shape.

Small sinter precipitates from sinter basins

At locality 6 (Fig. 4) crystal rafts, several centimeters in diameter are observed. These single crystal aggregates are characterized by a planar upper boundary at the air-water interface and a rhombohedral boundary downward (Fig. 7a and b) extending into the pool water. At the edge of the sinter basins, above the present water level, ancient raft deposits are attached to flowstones (cp. Fig. 4). The morphology of these pool calcites, characterized by acute rhombohedral faces at the flanks and obtuse rhombohedral faces at their growth ends (Fig. 7a and b), are similar to calcite precipitates (Fig. 7c and d) on watch-glasses placed during monitoring experiments in the Bunker Cave (Northern Sauerland/NRW; Riechelmann, 2010).

4.2 Carbon and oxygen isotopic composition

Isotope analysis reveals a distinct difference in the signature of host limestone and speleothems samples. Host limestone samples exhibit δ^{13}C values between +1.8 and +2.7‰ and δ^{18}O values between −5.3 and −1.0‰. These values are characteristic for the typical carbon and oxygen isotopic compositions of Middle/Upper Devonian limestones of the Rhenish Slate Mountains (Fig. 8).

Rhombohedral crystal sinters as well as spherulitic crystal sinters collected at the cave floor and on collapsed blocks display δ^{13}C values between +0.6 and −7.3‰ and δ^{18}O values between −6.9 and −18.0‰ (Fig. 8). Carbon versus oxygen isotope

TCD
4, 1011–1034, 2010

plots reveal an overall trend towards elevated carbon and depleted oxygen ratios. In essence, spherulitic crystal sinters represent the depleted δ^{18}O end-member whereas translucent rhombohedral crystal sinters (type a) are characterized by ^{18}O-enriched values close to those measured from stalagmites, stalactites or sinter curtains collected in the "Herbstlabyrinth" cave system (Fig. 8). Buff-colored rhombohedral crystallites form a slightly enriched δ^{18}O cluster, relative to spherulitic crystal sinters. Composite crystallites, built by nuclei of translucent rhombohedral crystal sinters and white to buff-colored rhombohedral cortices are located in a geochemical transition zone between type a and type b rhombohedral crystal sinters.

The rafts of the sinter basin of locality 6 show δ^{13}C values ranging between −10.8 and −10.3‰ and δ^{18}O values between −6.5 and −6.4‰. These values match those obtained from stalagmites, stalactites or sinter curtains sampled in the "Herbstlabyrinth" (Fig. 8).

4.3 U/Th age dating

TIMS U/Th age dating of "crystal sands" collected in the "Rätselhalle" were performed in the laboratory of A. Eisenhauer (Leibniz Institute of Marine Sciences, Kiel) suggested 29 170 ± 480 yrs (Kempe et al., 2005). According to Kempe (2008), the dated material belongs to the most common type of crystals, the type a of the rhombohedral crystal sinter as described here. Similar age data of 28 700 ± 1500 yrs BP were obtained by TIMS U/Th age dating of aggregates of type b (white to buff-coloured, rhombohedral crystal) sinters at the Research Centre for Radiometry; Heidelberg Academy of Sciences (laboratories of A. Mangini and R. Eichstädter). As SEM studies revealed an overgrowth of type a by type b and as these two precipitates could not be separated mechanically or chemically prior to U/Th analysis, the resulting age data of 28 700 ± 1500 yrs are likely to underestimate the precipitation age of type b rhombohedral crystals.

TCD
4, 1011–1034, 2010

5 Discussion

The accumulations of unconsolidated crystallites in the cave under study are exclusively characterized by calcite morphologies with rhombohedral faces of different steepness. According to Gonzales et al. (1992), this is a typical feature of cave-related calcite precipitation. Similarly, calcite crystals with acute rhombohedral faces on the edges and obtuse rhombohedral faces at their free ends have been described by Mergener et al. (1992) from sinter basins of several caves of the Sauerland (NE Rhenish Slate Mountains).

Crystallites of this type dominate aggregates of "crystal sands" at locality 1 as well as recent to sub-recent sinter basin precipitates (loc. 6) on pool walls and floors. Moreover, this type occurs below rafts up to a paleo-water level mark characterized by a shelfstone mark 10 cm above the present-day water level. There is no field or petrographic evidence, however, suggesting that fluctuating paleo-water levels in the cave represent controlling factors for formation of crystal accumulations and other modes of formation are consequently discussed. Perhaps the main lines of evidence comes from differential isotopic signatures of these precipitates in comparison to other speleothem precipitates allowing for an interpretation of the formation conditions of calcites in sinter basins under specific physicochemical conditions (Žák et al., 2004, 2008; Richter and Niggemann, 2005; Lacelle, 2007). Below geochemical evidence is presented in overview and discussed in its overall context:

1. The calcites of recent and subrecent rafts are isotopically depleted relatively to normal speleothems (Fig. 8). This is perhaps best understood in the context of their precipitation in pools fed by drip water as opposed to crystallization on stalagmite surfaces under a semi-permanent, thin water film. In addition, evaporation processes play an important role on stalagmite and stalactite surfaces including kinetic effects related to CO_2 degassing (Mickler et al., 2006). In contrast, these effects are far less significant in permanently water filled cave pools.

TCD
4, 1011–1034, 2010

2. The aggregates of translucent calcites with acute and obtuse rhombohedral crystal faces plot, in terms of their isotope signature, at the fringes of the isotopic range defined by normal speleothems. Elevated carbon and depleted oxygen-isotope values are probably indicative for less soil zone activity and a rather scarce vegetation cover related to overall cooler climates in comparison to the present-day setting.

3. The calcite particles with obtuse and curved rhombohedrons reveal ^{13}C enriched and ^{18}O depleted signatures relative to precipitates mentioned under 1 and 2 (see above). This is considered evidence for precipitation in gradually freezing residual water. During this process, ^{18}O was preferentially incorporated in the newly formed ice (O'Neil, 1968; Clark and Fritz, 1997).

4. Acute clear rhombohedrons with coatings of buff-colored rhombohedrons (cp. Figs. 5f and 6c, d) range, in terms of their isotopic signature between the calcites described in 2 and 3 (see above). These precipitates may indicate the initial freezing of pool waters.

5. Individual spherulites and spherulitic structured braid sinters reveal the highest carbon and the lowest oxygen isotope composition relative to other particles of the "crystal sands". This is considered evidence for the final freezing stages of the pool waters.

Based on arguments brought forward in the previous text, crystal precipitates as well as crystal aggregates accumulated in "crystal sands" of the "Rätselhalle" are placed in a tentative genetic succession. Based on this, a series of climate stages (I to VI in Fig. 9) results that is placed in its temporal context using the U/Th age data obtained from acute clear rhombohedral calcites (Kempe et al., 2005; 29 170 ± 480 yrs BP):

I. Permafrost stage prior to Weichselian interstadial 4 (terminology in accordance with Johnsen et al., 1992 and Bond et al., 1997); no sinter formation is recorded.

TCD
4, 1011–1034, 2010

II. Beginning of cave ice formation when the 0 °C isotherm reaches the roof of the cave during the beginning of Weichselian interstadial 4. The precipitation of small calcite crystals from rapidly freezing of dripping water conceivable but evidence is not yet found.

III. Residual ice on cave ground during the Weichselian interstadial 4 still exists. Sintering of debris on ice along the cave walls ("ice attachments") takes place and precipitation of crystallites with isotopic signatures that overlap with those of stalagmites and stalactites occurs in meltwater pools on ice.

IV. Slow freezing of water in pools on the ice bodies in the cave during cooling at the beginning of renewed permafrost conditions following Weichselian interstadial 4. Cryogenic calcites precipitate from slowly freezing pool water.

V. Permafrost after Weichselian interstadial 4 inhibits crystal precipitation as all water in the cave is frozen.

VI. A renewed stage of interglacial climate follows the permafrost interval. Ice bodies in caves melt and cryogenic and other speleogenic particles accumulate in an unsorted manner on the cave floor or cover collapse blocks.

The isotopic composition of genetically different, small cryogenic sinters (rhombohedral crystal sinters, spherulitic sinters) found in the "Rätselhalle" ranges from the typical $\delta^{18}O$ and $\delta^{13}C$ signature of normal speleothems to ^{13}C enriched and ^{18}O depleted signatures of cryogenic calcites (see arrow B-C in Fig. 8). A compilation of the published data on slowly precipitating cryocalcites from various Central European caves is indicative of a cave or locality-specific isotope signature (Fig. 10). This implies cave specific climate conditions. Žák et al. (2004) and Richter et al. (2009a) propose enhanced ventilation of the cave or of portions of a given cave resulting in a trend towards elevated $\delta^{13}C$, this because degassing CO_2 is increasingly removed under increasing ventilation. This is important for the initial point of cryogenesis of the calcites of the various caves.

TCD
4, 1011–1034, 2010

6 Conclusions

In conclusion, the need for more research of the often highly complex cryogenic calcites in caves of the Rhenish Slate Mountains and in other localities is great. Specifically, attention should be paid to overgrowth of younger precipitation phases on nuclei of older ones. Furthermore, different generations of cryogenic calcites must be separated in terms of their mineralogy, crystallography and geochemical signature. If successful, the combination of palaeo-environmental information from cave climate archives, precipitated during interglacials with evidence from cryogenic calcites allows for a much improved reconstruction of the Pleistocene/Holocene climate evolution of Central Europe.

Acknowledgements. Technical support we owe to the staff of the institute for Geology, Mineralogy and Geophysics of the Ruhr-University Bochum – B. Gehnen (C-O isotope chemistry), R. D. Neuser (SEM) (Bochum). The TIMS U/Th-age determination were made by the kind and generous R. Eichstädter at the research centre of radiometry of the Heidelberg Academy of Science. We express our thanks to reviewers for constructive comments.

References

Bond, G., Showers, W. J., Cheseby, M., Lotti, R., Almasi, P., deMenocal, P., Priore, P., Cullen, H., Hajdas, I., and Bonani, G.: A pervasive millennial-scale cycle in North Atlantic Holocene and glacial climates, Science, 278, 1257–1266, 1997.

Clark, I. D. and Fritz, P.: Environmental Isotopes in Hydrogeology, CRC Press, Lewis Publishers, Boca Raton, FL, 1997.

Dorsten, I., Hülsmann, T., and Hüser, A.: Das Herbstlabyrinth-Adventhöhlensystem – die erste Riesenhöhle Hessens, Mitt. Verb. dt. Höhlen- u. Karstforsch., 51, 4–10, 2005.

Erlenmeyer, M., Hasenmeyer, B., and Schudelski, A.: Das Höhlensystem Kreishalle-Malachitdom – ein bemerkenswerter Aufschluss für Höhlenminerale, in: Der Malachitdom – Ein Beispiel interdisziplinärer Höhlenforschung im Sauerland, Geologisches Landesamt Nordrhein-Westfalen, Krefeld, 69–89, 1992.

TCD
4, 1011–1034, 2010

Füchtbauer, H. and Richter, D. K.: Karbonatgesteine, in: Sedimente und Sedimentgesteine, 4. Edn., edited by: Füchtbauer, H., E., Schweiz, Verlagsbuchhandlung (Naegele u. Obermiller), Stuttgart, 233–434, 1988.
Gonzalez, L. A., Carpenter, S. J., and Lohmann, K. C.: Inorganic calcite morphology; roles of fluid chemistry and fluid flow, J. Sediment. Res., 62, 382–399, 1992.
Grubert, C.: Neuland in Hessen, Mitt. Verb. dt. Höhlen- u. Karstforsch., 42, 37, 1996.
Hülsmann, T.: Die Erforschung des Herbstlabyrinth-Adventhöhle-Systems, Jahresbericht 1996, Speläologische Arbeitsgemeinschaft Hessen e. V., 6–22, 1996.
Johnsen, S. J., Clausen, H. B., Dansgaard, W., Fuhrer, K., Gundestrup, N., Hammer, C. U., Iversen, P., Jouzel, J., Stauffer, B., and Steffensen, J. P.: Irregular glacial interstadials recorded in a new Greenland ice core, Nature, 359, 311–313, 1992.
Kaiser, T. M., Keller, T., and Tanke, W.: Ein neues pleistozänes Wirbeltiervorkommen im Paläokarst Mittelhessens (Breitscheid-Erdbach, Lahn-Dill-Kreis), Geol. Jb. Hessen, 126, 71–79, 1998.
Kayser, S.: Erläuterung zur geologischen Karte von Preussen, Lieferung 101, Blatt Herborn, 1–72, 1907.
Kempe, S., Doeppes, D., Bauer, I., Dirks, H., Dorsten, I., Hueser, A., and Eisenhauer, A.: Naturally damaged speleothems, indicators of glacial cave ice in Central Europe, Karst Waters Institute Special Publication, 10, 35, 2006.
Kempe, S.: Natürliche Sinterschäden, Indikatoren für glaziales Höhleneis in Mitteleuropa, Stalactite, 58, 39–42, 2008.
Krebs, W.: Der Bau des oberdevonischen Langenaubach-Breitscheider Riffes und seine Entwicklung im Unterkarbon (Rheinisches Schiefergebirge), Abh. Senkenberg, Naturforsch. Ges., 511, 1–105, 1966.
Krebs, W.: Devonian Reef Limestones in the Eastern Rhenish Schiefergebirge, Sedimentology of parts of Central Europe, edited by: Müller, G. and Friedman, G. M., Verlag Waldemar Kramer, Frankfurt am Main, Heidelberg, 1971.
Lacelle, D.: Environmental setting, (micro)morphologies and stable C-O isotope composition of cold climate carbonate precipitates; a review and evaluation of their potential as paleoclimatic proxies, Quaternary Sci. Rev., 26, 1670–1689, 2007.
Mergner, W., Brix, M. R., Hagemann, P., Oelze, R., and Richter, D. K.: Sinterbecken im Malachitdom mit wasserspiegelparallelen Karbonatkrusten, in: Der Malachitdom – Ein Beispiel interdisziplinärer Höhlenforschung im Sauerland, Geologisches Landesamt

TCD
4, 1011–1034, 2010

Nordrhein-Westfalen, Krefeld, 151–173, 1992.
Mickler, P. J., Stern, L. A., and Banner, J. L.: Large kinetic isotope effects in modern speleothems, Geol. Soc. Am. Bull., 118, 65–81, 2006.
O'Neil, J. R.: Hydrogen and oxygen isotope fractionation between ice and water, J. Phys. Chem., 72, 3683–3684, 1968.
Richter, D. K. and Niggemann, S.: Kryogene Calcite in Höhlen des Rheinischen Schiefergebirges, Mitt. Verb. dt. Höhlen- u. Karstforsch., 51, 129–132, 2005.
Richter, D. K., Neuser, R. D., and Voigt, S.: Kryogene Calcitpartikel aus der Heilenbecker Höhle in Ennepetal (NE Bergisches Land/Nordrhein-Westfalen), Die Höhle, 59, 37–47, 2008.
Richter, D. K. and Riechelmann, D. F. C.: Late Pleistocene cryogenic calcite spherolites from the Malachitdom Cave (NE Rhenish Slate Mountains, Germany); origin, unusual internal structure and stable C-O isotope composition, Int. J. Speleol., 37, 119–129, 2008.
Richter, D. K., Voigt, S., and Neuser, R. D.: Kryogene Calcite unterschiedlicher Kristallform und Kathodolumineszenz aus der Glaseishöhle am Schneiber (Steinernes Meer/Nationalpark Berchtesgaden, Deutschland), Die Höhle, 60, 3–9, 2009a.
Richter, D. K., Dreyer, R., Niggemann, S., and Pielsticker, K.-H.: Kryocalcite in der Großen Sunderner Höhle (Sauerland) – ein weiterer Beleg für die vormalige Eishöhle, Mitt. Verb. dt. Höhlen- u. Karstforsch., 55, 80–85, 2009b.
Riechelmann, D. F. C.: Aktuospeläologische Untersuchungen in der Bunkerhöhle des Iserlohner Massenkalks (NRW/Deutschland): Signifikanz für kontinentale Klimaarchive, Ruhr-Universität Bochum, Bochum, 198 pp., in preparation, 2010.
Spötl, C.: Kryogene Karbonate im Höhleneis der Eisriesenwelt, Die Höhle, 59, 26–36, 2008.
Stengel-Rutkowski, W.: Karsterscheinungen im oberdevonischen Riffkalkstein (Iberger Kalk) von Erdbach und Breitscheid (Dillmulde, Rheinisches Schiefergebirge), Mitt. Verb. dt. Höhlen- u. Karstforsch., 14, 75–80, 1968.
Žák, K., Urban, J., Cilek, V., and Hercman, H.: Cryogenic cave calcite from several Central European caves; age, carbon and oxygen isotopes and a genetic model, Chem. Geol., 206, 119–136, 2004.
Žák, K., Onac, B. P., and Peroiu, A.: Cryogenic carbonates in cave environments: a review, Quatern. Int., 187, 84–96, 2008.

TCD
4, 1011–1034, 2010

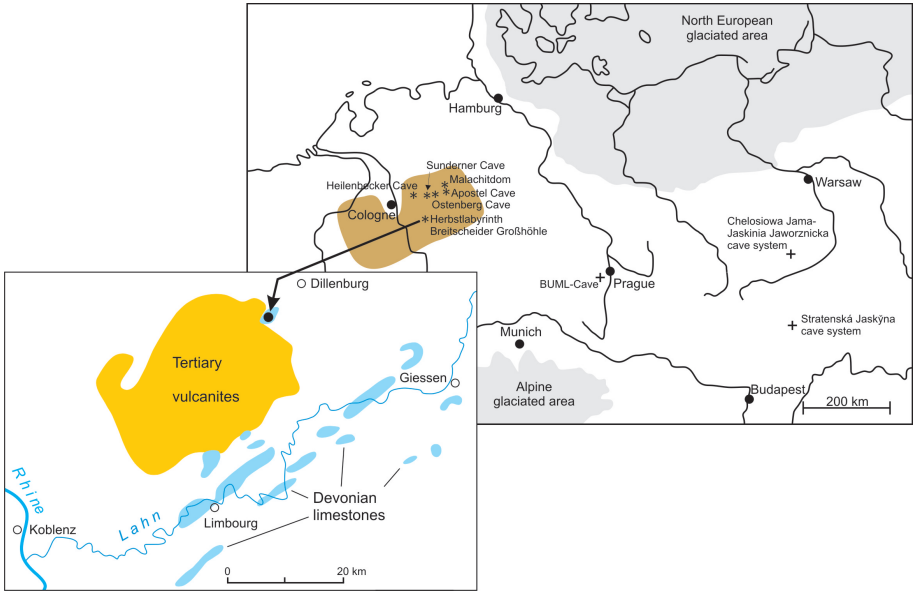

Fig. 1. Map showing the position of the "Breitscheider Großhöhle" as well as the other caves of Central Europe from which cryocalcites have been described. See lower left inset for more details.

TCD
4, 1011–1034, 2010

Fig. 2. Sketch map of "Breitscheider Großhöhle" showing position of "Rätselhalle". For sampling localities refer to Fig. 4.

TCD
4, 1011–1034, 2010

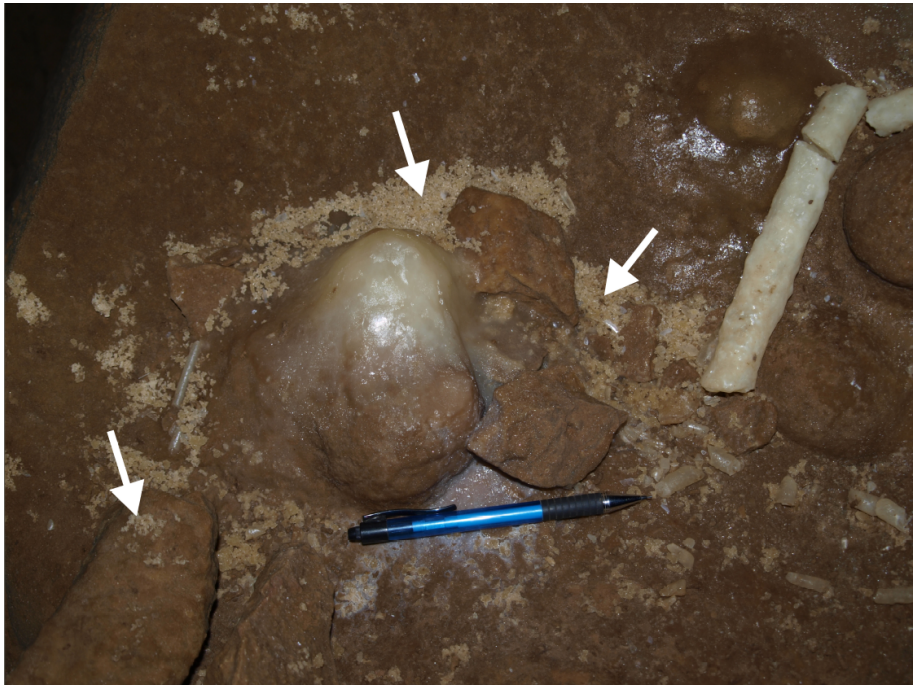

Fig. 3. Crystal sand accumulates on collapse block (see arrows) in the “Rätselhalle”.

TCD
4, 1011–1034, 2010

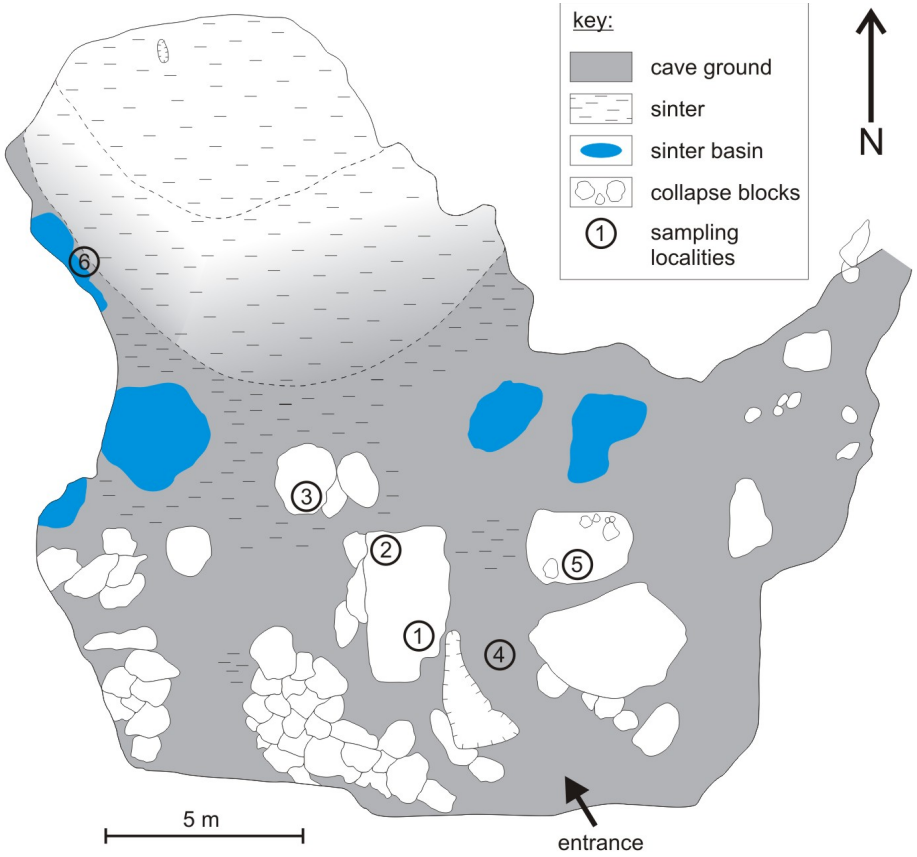

Fig. 4. Speleological map of the "Rätselhalle" with indication of sampled locations.

TCD
4, 1011–1034, 2010

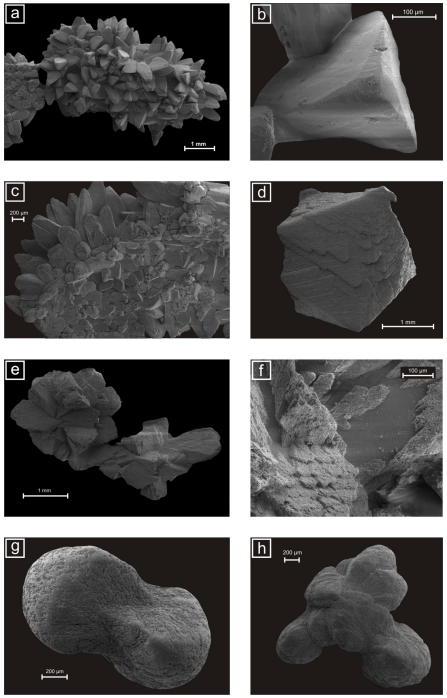

Fig. 5. SEM images of various types of crystal sands. **(a)** Surface of a sinter platelet (central particle) with translucent rhombohedral crystals (acute rhombohedral faces on the flanks, obtuse rhombohedral faces at growth end); particles to the left mark bottom of sinter platelet. **(b)** Growth end of a translucent rhombohedral crystal with obtuse rhombohedral faces at the apex area of the crystal. **(c)** Moderately curved bottom of a sinter platelet with translucent rhombohedral crystals. (**d** and **e**) Rhombohedral crystal sinters (whitish to buff-colored) without acute rhombohedral faces but with distinct domain development; (d)=single crystals, (e)=chain. **(f)** Partial overgrowth of translucent rhombohedral crystal sinter (type a; smooth surfaces) by rhombohedral crystal sinter (type b) with a distinct domain growth. **(g)** Dumbbell-shaped spherulithic crystal sinter. **(h)** Braided shaped spherulitic crystal sinter.

TCD
4, 1011–1034, 2010

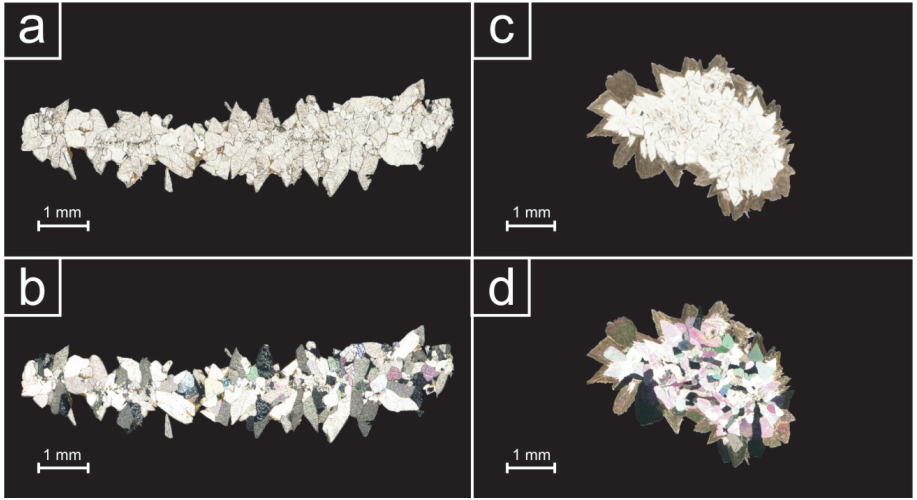

Fig. 6. Thin section photomicrographs of rhombohedral crystal sinters of the crystal and at locality 1: (**a** and **b**) – sunken rafts with rhombohedral crystals on both sides (b – with crossed polarizers). (**c** and **d**) – Calcitic aggregates with translucent crystals in the interior and with darker (inclusion-rich) overgrowth (d – with crossed polarizers).

TCD
4, 1011–1034, 2010

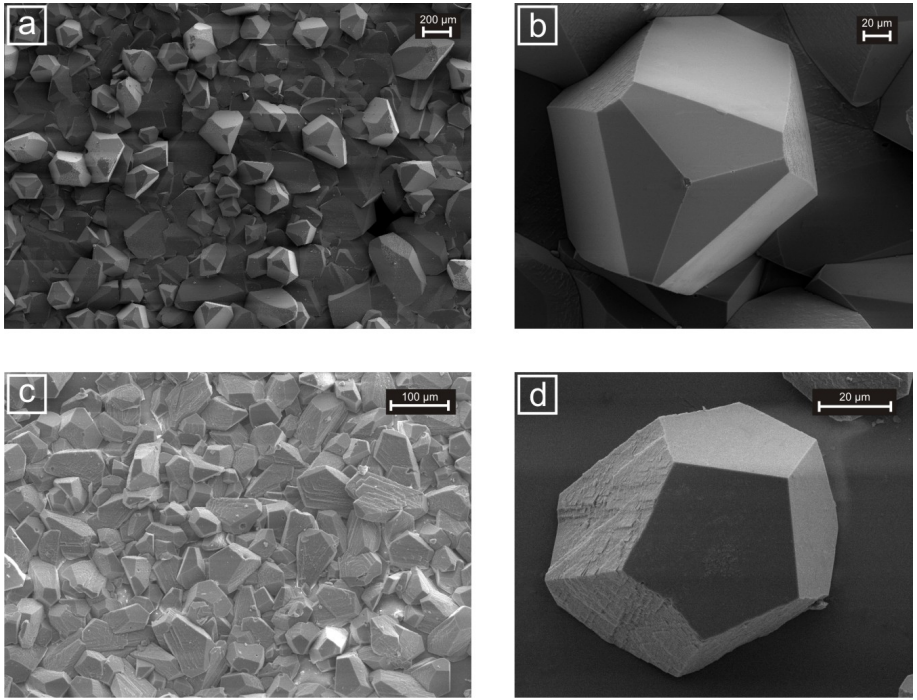

Fig. 7. **(a)** Crystal lawn (precipitated into basin) with acute rhombohedral faces on the flanks and obtuse rhombohedral faces at growth end. Subrecent rafts collected at locality 6 (Fig. 4b) detailed view of a single crystal shown in (a). **(c)** Calcites of watch glasses, placed on top of stalagmites in the Bunker Cave (Riechelmann, 2010). **(d)** detailed view of a single crystal shown in (c).

TCD
4, 1011–1034, 2010

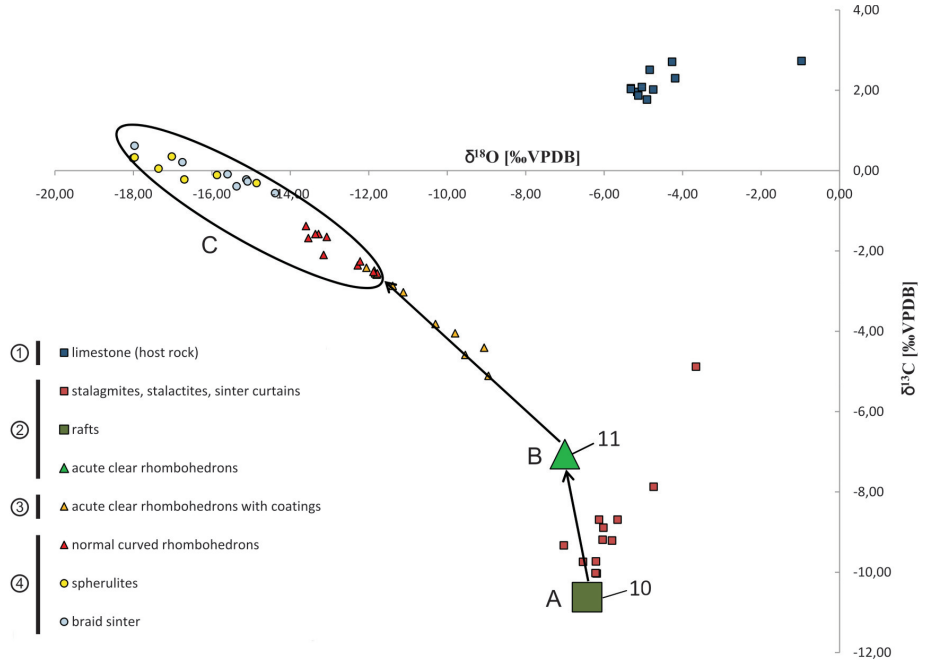

Fig. 8. Carbon and oxygen isotopic composition of various calcite particles of the "Rätselhalle" in comparison to those measured from calcitic host rock samples (1) and calcites of stalagmites, stalactites and sinter curtains (2). (3) normal calcites overgrown by cryogenic calcites, (4) cryogenic calcites.

TCD
4, 1011–1034, 2010

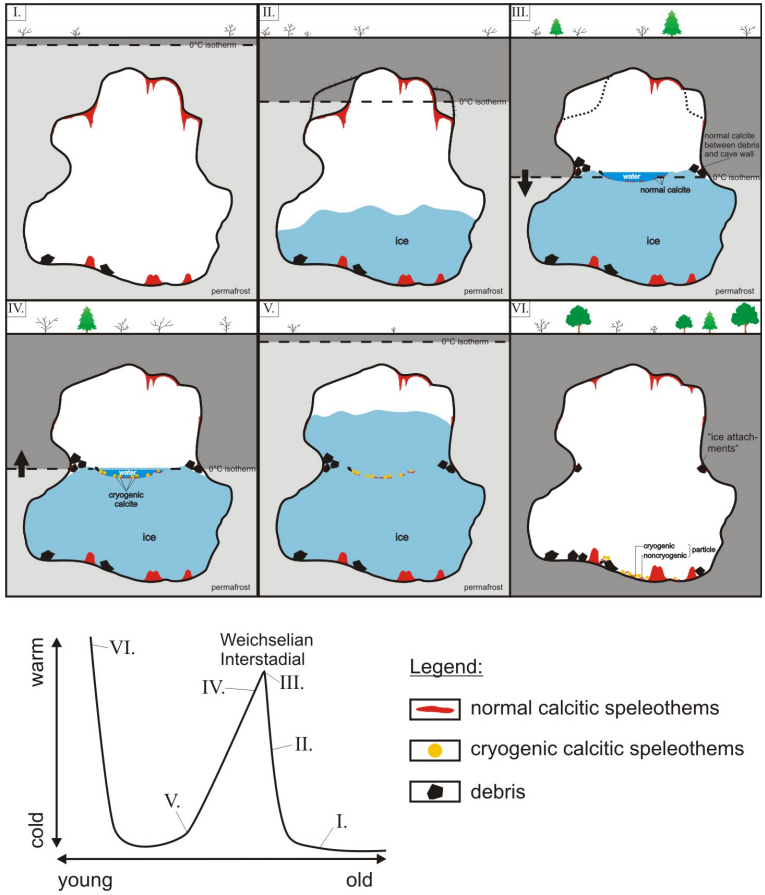

Fig. 9. Cartoon illustrating proposed succession of events that lead to the formation of cryogenic and non-cryogenic calcites in the course of a Weichselian interstadial. Refer to schematic temperature evolution in lower left inset. See text for explanations.

TCD
4, 1011–1034, 2010

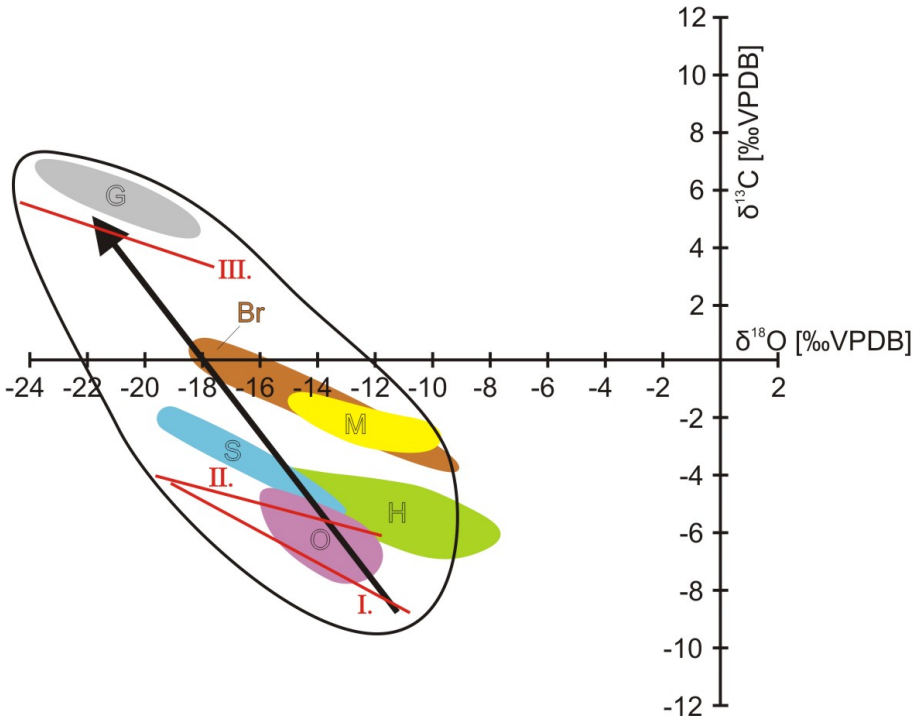

Fig. 10. Carbon and oxygen isotopic composition of cryogenic calcites from various cave localities in Central Europe: I–III=regression line – Žák et al. (2004); I. "Jaskinia Jaworznicka" Cave system; II. "BUML"-Cave; III. "Stratenská Jaskya" Cave. The different data clouds are based on the interpretation by the Bochum group. O="Ostenberg" Cave – Richter and Niggemann (2005); S="Sunderner" Cave – Richter et al. (2009a); H="Heilenbecke" Cave – Richter et al. (2008); M="Malachitdom" – Richter and Riechelmann (2008); Br="Breitscheid-Erdbach" Cave – this work, G="Glaseis" Cave – Richter et al. (2009b).

TCD
4, 1011–1034, 2010